frontiers | Frontiers in Energy Research

TYPE Original Research
PUBLISHED 29 December 2023
DOI 10.3389/fenrg.2023.1313451

OPEN ACCESS

EDITED BY
Dongfang Yang,
National Research Council Canada (NRC), Canada

REVIEWED BY
Xiaohui Yan,
Shanghai Jiao Tong University, China
Ugur Pasaogullari,
University of Connecticut, United States
Zhenye Kang,
Hainan University, China

*CORRESPONDENCE
Yulin Wang,
wangylfcs@gmail.com

RECEIVED 10 October 2023
ACCEPTED 29 November 2023
PUBLISHED 29 December 2023

CITATION
Li H, Huang S, Guan C, Wang H, Nakajima H, Ito K and Wang Y (2023), Experimental optimization of the Nafion® ionomer content in the catalyst layer for polymer electrolyte membrane water electrolysis at high temperatures.
Front. Energy Res. 11:1313451.
doi: 10.3389/fenrg.2023.1313451

Experimental optimization of the Nafion® ionomer content in the catalyst layer for polymer electrolyte membrane water electrolysis at high temperatures

Hua Li[1], Senrui Huang[1], Chao Guan[2], Huixuan Wang[2], Hironori Nakajima[3], Kohei Ito[3] and Yulin Wang[1,2]*

[1]Ningbo Institute of Material Technology and Engineering, Chinese Academy of Sciences, Ningbo, China, [2]Tianjin Key Lab of Refrigeration Technology, Tianjin University of Commerce, Tianjin, China, [3]Department of Hydrogen Systems, Graduate School of Engineering, Kyushu University, Fukuoka, Japan

The polymer electrolyte membrane water electrolysis (PEMWE) performance is closely related to the Nafion® ionomer content in catalyst layers (CLs). This study experimentally investigates the impact of anode and cathode Nafion® ionomer contents on the PEMWE performance at high temperatures. The Nafion® ionomer content is 5–30 wt% on both anode and cathode sides, while the temperature and operating pressure change from 80°C to 120°C and 0.1 MPa to 0.3 MPa, respectively. Experimental results reveal that elevated temperature and operating pressure can remarkably promote the performance of PEMWE with a reasonable Nafion® ionomer content and without dehydrating the membrane at 120°C and 0.3 MPa. However, the PEMWE performance deteriorates as the Nafion® ionomer content is too low. The anode Nafion® ionomer content has a relatively great impact on ohmic resistance, concentration, and activation overpotential, especially the concentration overpotential. Nevertheless, the cathode Nafion® ionomer content only affects the ohmic resistance. Finally, under the operating conditions of 120°C and 0.3 MPa, employing a Nafion ionomer content of 10 wt% in the anode–cathode sides minimizes the electrolysis voltage to 2.18 V at 18 A/cm^2.

KEYWORDS

polymer electrolyte membrane water electrolysis, Nafion® ionomer content, high temperature, operating conditions, performance of polymer electrolyte membrane water electrolysis

1 Introduction

Renewable energy sources may resolve energy and environmental problems and create a highly developed energy civilization. However, renewable energies are often limited by the parameters of time and place, and the sources are heterogeneously distributed (Wang et al., 2019; Wang et al., 2023; Wang et al., 2024). Hydrogen produced by water electrolysis is deemed to be one solution to save these power sources. Polymer electrolyte membrane water electrolysis (PEMWE) yields high hydrogen purity, improved safety and dependability, decreased energy consumption, and the potential for high current density; therefore, PEMWE has acquired substantial consideration (Carmo et al., 2013; Park et al., 2021). Nevertheless, PEMWE still suffers from high market cost (Awasthi et al., 2011; Chandesris et al., 2015; Feng et al., 2017; Wang et al., 2022) because PEMWE uses a noble metal catalyst and expensive perfluorosulfonic acid (PFSA) membranes (Feng et al., 2017; Siracusano et al., 2017; Teuku et al., 2021).

To reduce the high cost of PEMWE, one method is to compact the size by increasing the current density. Various parameters that impact the current density of PEMWE have been investigated, such as operation temperature and pressure (Xu et al., 2011; Xu et al., 2012; Xu et al., 2014; Li et al., 2016a; Lee et al., 2016; Stiber et al., 2021), properties of the anode and cathode porous transport layers (PTLs) (Ito et al., 2012; Li et al., 2016b; Li et al., 2018; Kroschel et al., 2019; Doan et al., 2021), and properties of the anode and cathode catalyst layers (CLs) (Natarajan et al., 2013; Lee et al., 2016; Holzapfel et al., 2020; Lopata et al., 2020; Pham et al., 2021). Recently, optimizing CLs has attracted the attention of many researchers because CLs directly affect the electrolysis performance and determine the durability and cost of PEMWE. In PEMWE, CLs usually consist of only two components: noble metal catalysts (such as IrO_2 or Pt/C) and ionomers (such as Nafion® ionomers). The ionomer content in CLs largely impacts the PEMWE performance because the ionomer in the CL functions as 1) a proton conductor, 2) an adhesive between CLs and the membrane, and 3) a hydrophilic agent to retain moisture and prevent membrane dehydration (Wang et al., 2020; Chen et al., 2021; Knöppel et al., 2021; Krivina et al., 2021).

Researchers have sought to optimize CLs by optimizing the Nafion® ionomer content in PEMWE at conventional temperatures (Xu and Scott, 2010; Su et al., 2013; Bernt and Gasteiger, 2016; Faid et al., 2020; Liu and Weber, 2022). They reported that there was an optimal ionomer content for the total electrolysis overpotential and nonlinear overpotential (activation or concentration overpotential). These studies also revealed that a decreased ionomer content in CL might decrease the proton conductivity of CLs but increase the real activation catalyst area. For example, Su et al. (2013) reported that the optimal Nafion® ionomer content in the anode side was 5–10 wt % when IrO_2 was employed. Bernt and Gasteiger (2016) examined the influence of the ionomer content on IrO_2/TiO_2 anode electrodes for PEMWE and found that the best performance was obtained for an ionomer content of 11.6 wt%. Xu and Scott (2010) revealed that the optimal contents of Nafion ionomer were 25% and 20% for anode and cathode CLs, respectively, when Ir–Ru was used. In addition, Su et al. (2013) and Xu and Scott (2010) reported that there should also exist an optimal Nafion® ionomer content for linear overpotential (ohmic overpotential). They expected that an increase in the Nafion® ionomer content would result in a decrease in the contact ohmic resistance between CLs and PEMWE, but it would also decrease electron conductivity due to the Nafion® ionomer that covers the catalyst particles. However, such an expectation of an ohmic overpotential still lacks experimental proof.

Moreover, most present researchers only concentrated on examining the effect of ionomer content on PEMWE performance under low temperature (80°C) (Xu and Scott, 2010; Su et al., 2013; Bernt and Gasteiger, 2016; Faid et al., 2020; Liu and Weber, 2022). Nevertheless, the effect of Nafion® ionomer content on PEMWE performance under high temperature may be different from that under conventional temperature. High temperatures tend to enlarge the current density by suppressing the overpotential (Xu et al., 2011; Li et al., 2016a) and soften the Nafion® ionomer, for which the glass transition temperature is lower than 130°C (Ito et al., 2011). Therefore, this study performed an experimental measurement to reveal the mechanism of how the ionomer content affected the PEMWE performance at high temperature and compared the results with those at conventional temperature. In addition, we attempt to optimize the Nafion® ionomer content on both anode and cathode sides for high-temperature PEMWE to compact its size by increasing the current density.

2 Experimental setup

The schematic diagram of the experimental system in this study and our previous studies (Li et al., 2016a; Li et al., 2016b) is displayed in Figure 1. The experimental system mainly includes a water tank with a capacity of 2 L, a water pump that exclusively feeds liquid deionized water to the anode side, a homemade PEMWE cell, two back pressure valves to regulate the operating pressure, two heaters to maintain the cell temperature, two mass flow meters to measure the flow rate of the generated gas, and two vapor traps to separate hydrogen and oxygen from water. Figure 1 shows a picture of testing equipment in the experimental system.

During the experiment, ohmic resistance and electrolysis voltage are measured using a high-frequency resistance (HFR) meter (frequency: 10 kHz; model: 356E; Tsuruga Electric Co., Japan). Every 1 s, a data logger records the HFR value, electrolysis voltage, and flow rates of hydrogen and oxygen at each current density point. Due to fluctuations, these four sets of data are calculated by averaging the data measured in 10 min. Moreover, these HFR values are measured after voltage stabilization (stable is defined as voltage fluctuations of not more than 3 mV in 10 min).

The water flow rate and cell temperature are precisely controlled because the current density is 0–18 A/cm². Membrane electrode assembly (MEA) heat generation can reach ~17 W/cm² at 18 A/cm² for high current densities, and the estimated water temperature elevation due to the produced heat is approximately 70°C at most; such high heat produced may overheat the membrane. For small current densities, a large water flow rate may decrease MEA temperature under the flow fields. Therefore, water is fed at approximately 20°C to prevent overheating of the membrane at high current densities, whereas the water flow rate is set at 1.0 mL/min to ensure sufficient time to heat the MEA temperature at a low current density. The utilization of water is 0.5% under the current density of 1 A/cm², whereas our previous study reported that the utilization of water is approximately 0.1% (Li et al., 2016a). A thermocouple is employed to measure the nominal temperature; the heater can automatically adjust the output power according to the flow field temperature to ensure that the temperature was kept unchanged during the measurement.

Figure 2 shows the schematic diagram and a picture of PEMWE in this experimental measurement. A Nafion® NRE-212-based catalyst-coated membrane (CCM) was sandwiched in between the anode and cathode sides of PEMWE; the current collectors in the anode side is made of a titanium mesh (NIKKO TECHNO, Japan), whereas that in the cathode side is manufactured with a carbon paper; serpentine flow-field plates are both employed on the anode and cathode plates. The above components are assembled together by bolts with an assembly pressure of 3 MPa. Table 1 shows the detailed

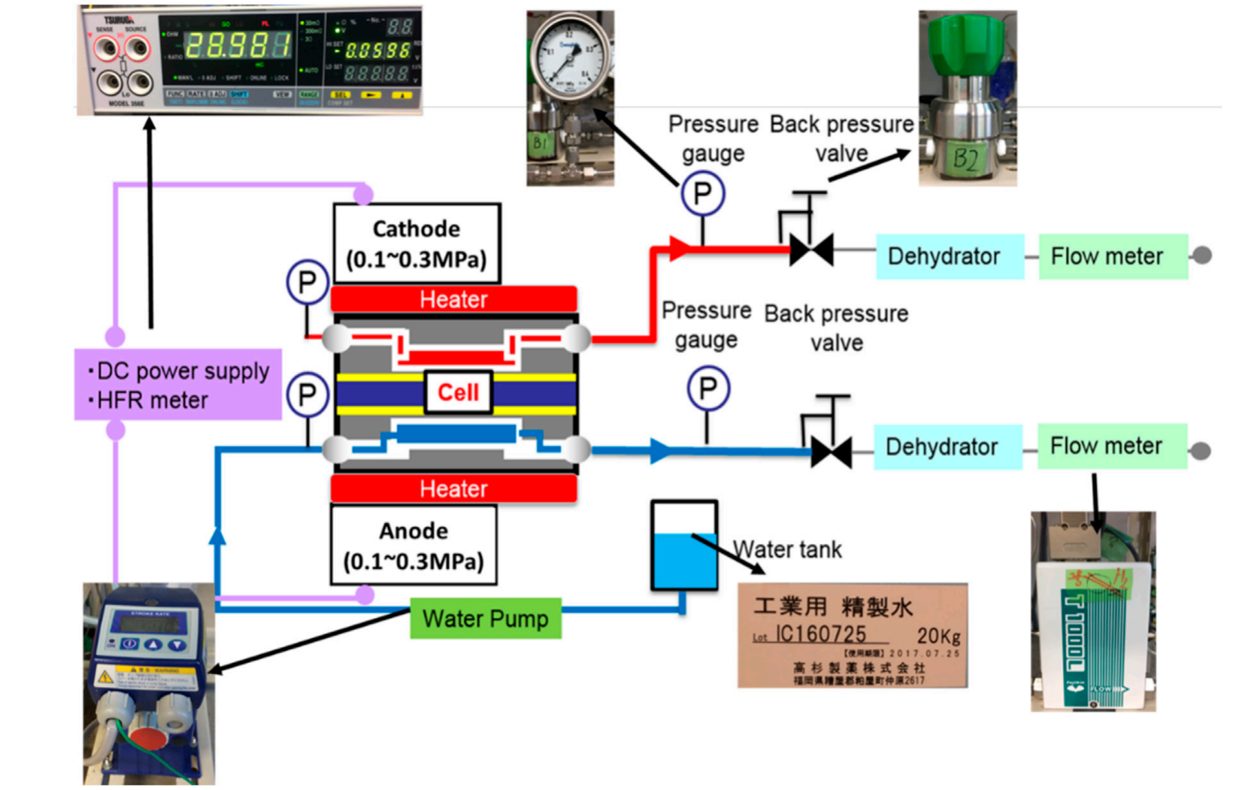

FIGURE 1
Schematic diagram of the experimental system for PEMWE at high temperatures.

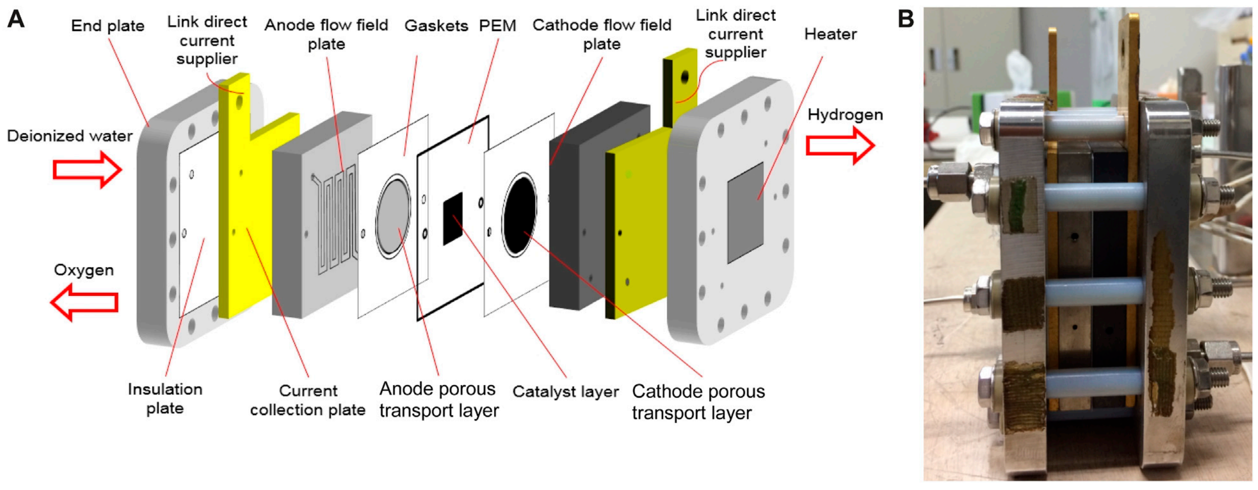

FIGURE 2
(A) Schematic diagram and **(B)** picture of PEMWE in this experimental measurement.

information of the operation conditions and components of PEMWE.

The spraying and hot-pressing approach was employed to manufacture CCM. The loading amount of IrO_2 and Pt (46 wt%, Pt/C) was 1.5 mg IrO_2/cm^2 and 0.5 mg Pt/cm^2 in the anode and cathode sides, respectively. All homemade CCMs were fabricated using the following process: any organic and inorganic contaminants with the PEMs of 64 cm^2 were removed prior to CCM manufacture (Ito et al., 2011) because those contaminants, such as Fe^{3+} and Mg^{2+}, accelerate the membrane degradation (Thanasilp and Hunsom, 2010). A slurry of catalyst and Nafion® ionomer (5 wt% Ion Power

TABLE 1 Properties and operation conditions of high-temperature PEMWE (Li et al., 2016a; Li et al., 2016b).

Component	Specification
Polymer electrolyte membrane (PEM)	Nafion® NRE-212, 88 cm^2
Anode CL	IrO_2, 1.5 mg IrO_2/cm^2
Cathode CL	Pt/C, 0.5 mg Pt/cm^2
Electrode area	1 cm^2
Anode material	Ti
Cathode material	Carbon
Channel width × height × length	1 mm × 1 mm × 33 mm
Pattern	Serpentine with 1-mm ribs
Anode porous transport layer	Ti sintered compact with Pt plating
	Porosity: 0.6
	Thickness: 0.2 mm
	Water contact angle: 0 (NIKKO TECHNO, JP)
Cathode porous transport layer	Carbon paper SGL34BA
	Porosity: 0.7
	Thickness: 0.3 mm
	Water contact angle: 120 (SGL Co., Germany)
Flow field plate	Titanium/carbon
Operation conditions	Temperature: 120
	Pressure: 0.3 MPa
	Water flow rate: 1 mL/min (only anode)

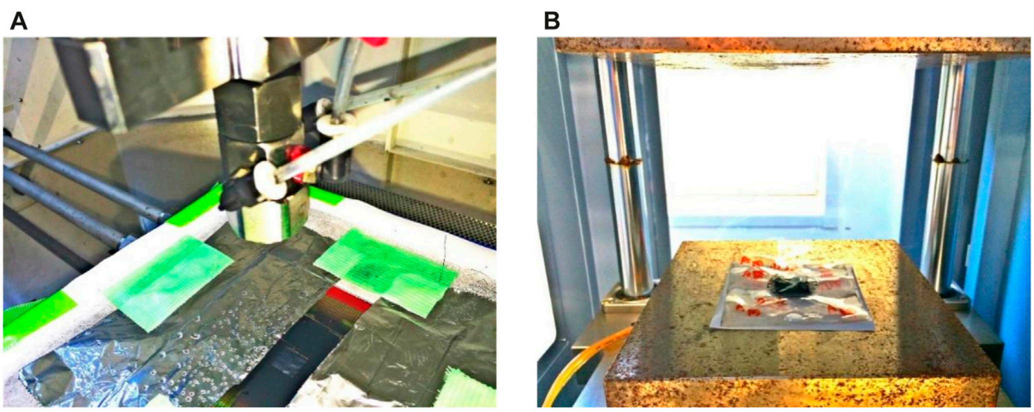

FIGURE 3
(A) Spraying of the catalyst ink onto the membrane and **(B)** hot pressing of the fabricated CCM.

solution) in deionized water and ethanol was prepared and sprayed onto one side of the membrane, as shown in Figure 3A. Finally, by hot pressing CCM at 2 MPa and 150°C for 180 s, the slurry was kept on the membrane, as shown in Figure 3B. Table 2 shows seven types of CCMs with different Nafion® ionomer contents in CLs.

TABLE 2 Properties of CCMs with different ionomer contents.

CCM number	1	2	3	4	3–1	3–2	3–3
Anode Nafion® ionomer content, wt%	30	20	10	5	10	10	10
Cathode Nafion® ionomer content, wt%	30	30	30	30	20	10	5

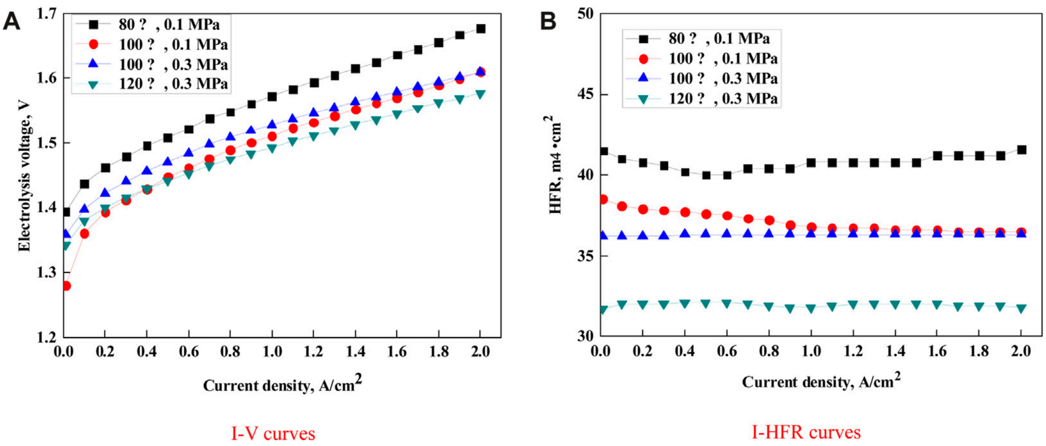

FIGURE 4
Curves of **(A)** I–V and **(B)** I–HFR at different increasing temperatures under the anode and cathode Nafion ionomer contents of 30 wt%.

3 Results and discussion

3.1 Impact of the elevated temperature

This section investigates the impact of elevated temperature on the I–V and I–HFR of PEMWE. Both the anode and cathode CLs have a Nafion ionomer content of 30 wt%. The elevated temperatures were 80°C–100°C and 100°C–120°C at 0.1 MPa and 0.3 MPa, respectively. Figure 4 shows that an elevated temperature benefits the water electrolysis performance, especially under a higher operating pressure. For instance, with temperature increasing from 80°C to 100°C at 0.1 MPa at a current density of 2 A/cm^2, the decrease in electrolysis voltage was 67 mV; however, when the temperature varied from 100°C to 120°C under 0.3 MPa, the electrolysis voltage reduced by 32 mV. Only elevating the operating pressure at conventional temperatures such as 100°C increased the open circuit voltage (OCV) but hardly affected the electrolysis voltage that was above 1.7 A/cm^2. In addition, the liquid–water phase could be enhanced with the increase in operating pressure, thereby preventing membrane dehydration, as observed in Figure 4B. Despite concerns over membrane dehydration by increasing temperature (Xu et al., 2011; Carmo et al., 2013; Chandesris et al., 2015), the membrane has not shown serious dehydration in the present range of temperature and pressure, as illustrated in Figure 4B. Increasing the temperature could reduce ohmic resistance and thus the electrolysis voltage, but the electrolysis voltage difference shown in Figure 4A is not only due to the decrease in ohmic overpotential but also due to the decrease in the activation overpotential (Xu et al., 2011; Carmo et al., 2013; Chandesris et al., 2015). After several hours of experimentation at 120°C and 0.3 MPa, the membrane of PEMWE showed little obvious dehydration. Therefore, the above operation conditions are employed in the following experiments.

3.2 Impact of the anode Nafion® ionomer content on the electrolysis performance

This section investigates the I–V characteristics, I–HFR characteristics, and IR–free voltage characteristics for CCM1, CCM2, CCM3, and CCM4 at 120°C and 0.3 MPa, as shown in Figure 5. I–HFR and IR–free voltage characteristics represent the resistance of ohmic and concentration polarization, which were employed to determine the linear overpotential and nonlinear overpotential. The nonlinear overpotential is equal to the left voltage after subtracting the linear overpotential from the electrolysis voltage.

Figure 5 shows that the optimal anode Nafion® ionomer content is 10 wt% (CCM3) for all of the I–V, I–HFR, and IR–free overpotential characteristics in this study. For example, PEMWE with CCM3 exhibits an ultra-high current density of 18 A/cm^2 at an electrolysis voltage of 2.18 V, as shown in Figure 5A. Therefore, the active area of the membrane and catalyst for PEMWE can be greatly reduced while maintaining a high-water-electrolysis performance. Moreover, PEMWE with CCM3 has the lowest ohmic resistances and smallest Tafel slopes, as shown in Figures 5B, C. In addition, the PEMWE cell operates without abnormal data for more than dozens of hours, which reflects that PEMWE with the Nafion® NRE-212 membrane can withstand high current densities at high temperatures.

Generally, the ohmic resistances of these four CCMs drop with an increase in current density, as shown in Figure 5B.

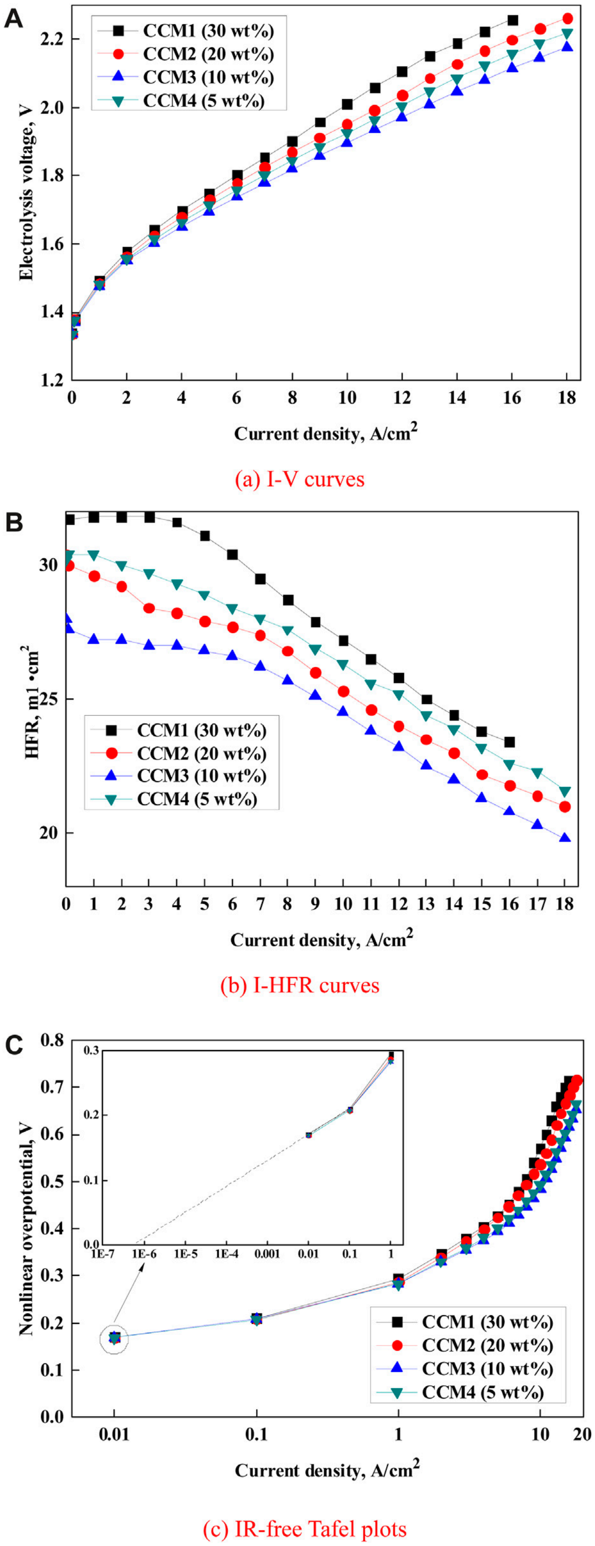

FIGURE 5
Curves of **(A)** I−V, **(B)** I−HFR, and **(C)** IR−free overpotential Tafel plots under different anode Nafion ionomer contents at 120°C and 0.3 MPa.

Because a higher current density yields a higher electro-osmosis drag force, more water molecules with protons can be drawn into the cathode side and reduce the ohmic resistance of CCMs. Figure 5B shows that ohmic resistance sharply increased when the Nafion® ionomer content reduced from 10 wt% to 5 wt%. This phenomenon has proved the aforementioned theoretical expectation: decreasing the ionomer content can increase the electron conductivity and the risk of separating the CL and membrane. Some researchers have reported that PEMWE showed good performance even with the anode Nafion® ionomer content of 0 wt% at conventional temperatures (Xu and Scott, 2010; Su et al., 2013; Bernt and Gasteiger, 2016; Faid et al., 2020). However, this study suggests maintaining at least 10 wt% Nafion® ionomer content for long PEMWE durability, especially at high temperatures.

In the IR−free overpotential Tafel plot, the slope of the linear part at a small current density represents the activation overpotential of every decade. Because the reactant supply is relatively sufficient at a small current density, the impact of reactant concentration can be negligible; therefore, the four CCMs with different Nafion® ionomer contents exhibit similar slopes of IR−free overpotential Tafel plots (Xu and Scott, 2010; Bernt and Gasteiger, 2016). This result indicates that the Nafion® ionomer content hardly affects the activation overpotential. However, at a high current density, the Tafel slopes denote the concentration overpotential. Nonlinear Tafel slope curves can be found for the four CCMs with different Nafion® ionomer contents. When the Nafion® ionomer content decreased from 30 wt% to 10 wt%, the sharp increase shifted toward the higher current density region. This behavior can be explained by the reduced catalyst particles covered by the ionomer with the decrease in the Nafion® ionomer content, as shown in Figure 6. The usual commercial IrO_2 actually contains both Ir(OH)x and IrO_2, which has a large and unevenly distributed volume gap. After a reasonable calcination, as shown in the red line of Figure 6C, the particles of IrO_2 tend to show a more uniform distribution with a small particle size, thereby leading to a high specific surface area of IrO_2, which favors the PEMWE performance. Therefore, more water can be electrolyzed, which decreases the nonlinear overpotential. Nevertheless, when the Nafion® ionomer content continuously decreased from 10 wt% to 5 wt%, the IR−free overpotential Tafel plots began to shift upward because an excessively low Nafion® ionomer content limited proton conductivity and increased the nonlinear overpotential. Overall, the Nafion® ionomer content impacts both linear and nonlinear overpotentials, as expected; however, the electrolysis voltage mainly depends on the nonlinear overpotential.

3.3 Impact of the cathode Nafion® ionomer content on the electrolysis performance

This section examines the impact of the cathode Nafion ionomer content on the PEMWE performance at 120°C and 0.3 MPa. The cathode Nafion ionomer content varied from 10 wt% to 30 wt%, whereas the anode Nafion ionomer content was maintained at 10 wt % based on the above result. Figure 7A shows that PEMWE with CCM3, CCM3-1, and CCM3-2 showed similar electrolysis voltages at current densities below 12 A/cm^2. However, at a current density above 12 A/cm^2, CCM3-1 and CCM3-2 had slightly lower

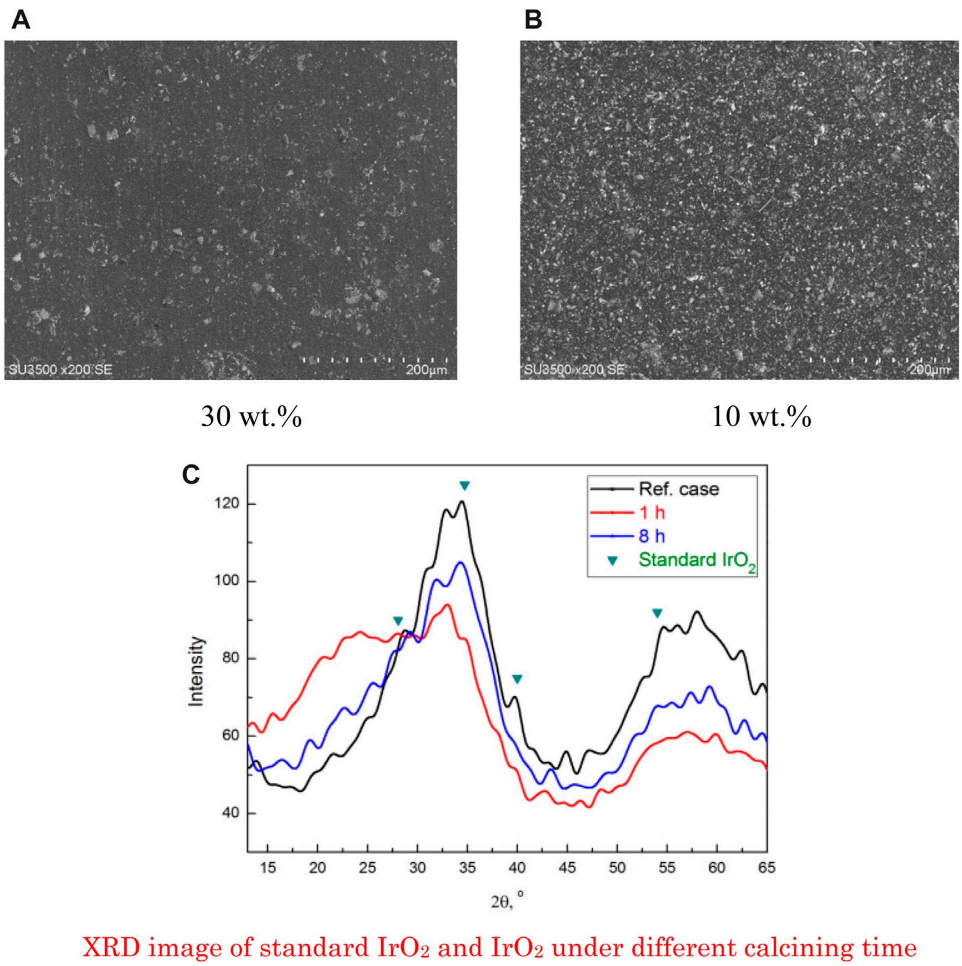

FIGURE 6
SEM image of the surface appearance of anode CLs with different Nafion® ionomer contents: **(A)** 30 wt% and **(B)** 10 wt% and **(C)** the XRD image of standard IrO_2 and IrO_2 under different calcining time.

electrolysis voltages than CCM3 due to the slightly higher HFR of the latter, as shown in Figure 7B. In addition, PEMWE with the cathode Nafion ionomer content of 5 wt% (CCM3-3) exhibited the worst electrolysis performance because the Nafion® ionomer content was too low, which limited proton conductivity and increased the nonlinear overpotential, as discussed above.

Figure 7B shows the I–HFR characteristics for PEMWE with CCM3, CCM3-1, CCM3-2, and CCM3-3. Similar to what was previously described, the HFR decreases with an increase in current density. In addition, the lowest HFR value was observed for CCM3-2 with a Nafion ionomer content of 10 wt%, while the HFR value increased when the ionomer content either decreased or increased with respect to this value. Bernt and Gasteiger (2016) suggested that in PEMWE, the increasing ionomer content would increase the contact resistance. The observation result of Figure 7B also identifies Bernt's conclusion. Moreover, the sudden increase in HFR in the 5 wt.% case is consistent with the prediction that ionomer functions as the binder between the CL and membrane. Figure 7C shows the IR–free overpotential Tafel plots for PEMWE with different cathode Nafion ionomer contents at different fixed current densities. The same IR–free overpotential plots and exchange current densities are observed for all current densities, which indicates that the cathode Nafion ionomer content hardly affects the activation overpotential and concentration overpotential.

4 Conclusion

This study experimentally investigated the impact of the Nafion® ionomer content in the anode and cathode CLs on the PEMWE performance at high temperature, and the following conclusions are obtained:

1) PEMWE with a Nafion® ionomer content of 10 wt% can significantly enhance the electrolysis performance at 120°C and 0.3 MPa compared to those at conventional and operating temperatures, whereas a too low content of the Nafion® ionomer introduces a sharp increase in ohmic resistance. Moreover, the membrane of the PEMWE cell exhibits no obvious dehydration at 120°C and 0.3 MPa.
2) The anode Nafion® ionomer content impacts both linear and nonlinear overpotentials. However, the nonlinear overpotential

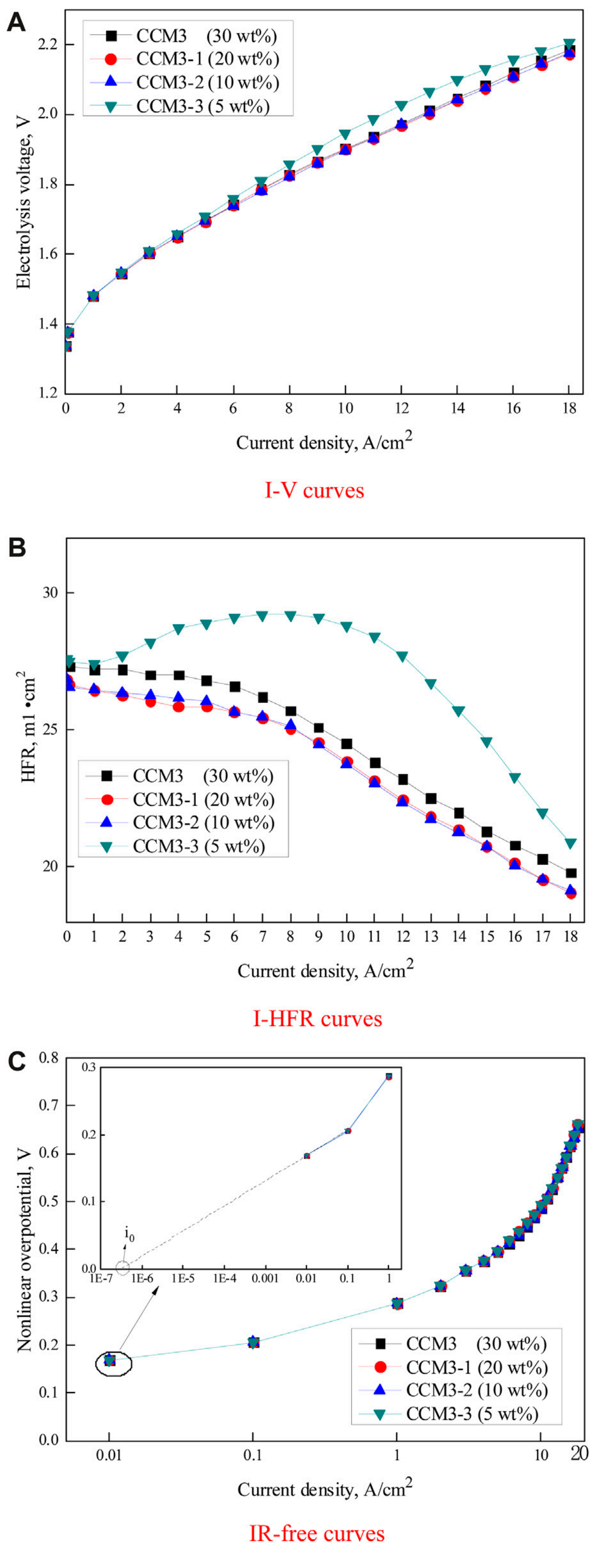

FIGURE 7
Curves of **(A)** I−V, **(B)** I−HFR, and **(C)** IR−free overpotential Tafel plots under different cathode Nafion ionomer contents at 120°C and 0.3 MPa.

contributes much more than the linear overpotential, and the maximum Nafion® ionomer content in the anode CL should be 10 wt% in this study.

3) The cathode Nafion® ionomer content affects only the ohmic resistance. Decreasing the Nafion® ionomer content can decrease the ohmic resistance by increasing the electron content, and the cathode Nafion® ionomer content should be 10 wt%.
4) Anode and cathode CLs employing a Nafion® ionomer content of 10 wt% can lead to a compact size of PEMWE by increasing the current density to 18 A/cm^2 at 2.17 V at 120°C and 0.3 MPa.

Data availability statement

The original contributions presented in the study are included in the article/Supplementary Material; further inquiries can be directed to the corresponding author.

Author contributions

HL: data curation, formal analysis, funding acquisition, investigation, methodology, resources, and writing–original draft. SH: investigation, methodology, software, and writing–review and editing. HN: conceptualization, investigation, supervision, and writing–review and editing. KI: conceptualization, data curation, investigation, supervision, and writing–review and editing. YW: data curation, funding acquisition, methodology, visualization, writing–original draft, and writing–review and editing.

Funding

The author(s) declare that financial support was received for the research, authorship, and/or publication of this article. The authors are grateful for the financial support from the National Natural Science Foundation of China (No. 52176084), the National Key Research and Development Program of China (No. 2022YFE0207600), the Yongjiang Talent Engineering Technology Innovation Team Project of Zhejiang Province, China (No. 2022A-008–C), the Zhejiang Key Laboratory of Advanced Fuel Cell and Electrolytic cell Technology (No. KLAFCET 202302), and the Tianjin Postgraduate Scientific Research Innovation Project (No. 2022SKYZ056). Tianjin Postgraduate Scientific Research Innovation Project (No. 2022SKYZ056) and National Key Research and Development Program of China (No. 2023YFB4005900).

Conflict of interest

The authors declare that the research was conducted in the absence of any commercial or financial relationships that could be construed as a potential conflict of interest.

Publisher's note

References

Awasthi, A., Scott, K., and Basu, S. (2011). Dynamic modeling and simulation of a proton exchange membrane electrolyzer for hydrogen production. *Int. J. hydrogen energy* 36 (22), 14779–14786. doi:10.1016/j.ijhydene.2011.03.045

Bernt, M., and Gasteiger, H. A. (2016). Influence of ionomer content in IrO2/TiO2 electrodes on PEM water electrolyzer performance. *J. Electrochem. Soc.* 163 (11), F3179–F3189. doi:10.1149/2.0231611jes

Carmo, M., Fritz, D. L., Mergel, J., and Stolten, D. (2013). A comprehensive review on PEM water electrolysis. *Int. J. hydrogen energy* 38 (12), 4901–4934. doi:10.1016/j.ijhydene.2013.01.151

Chandesris, M., Médeau, V., Guillet, N., Chelghoum, S., Thoby, D., and Fouda-Onana, F. (2015). Membrane degradation in PEM water electrolyzer: numerical modeling and experimental evidence of the influence of temperature and current density. *Int. J. Hydrogen Energy* 40 (3), 1353–1366. doi:10.1016/j.ijhydene.2014.11.111

Chen, F. Y., Wu, Z. Y., Adler, Z., and Wang, H. (2021). Stability challenges of electrocatalytic oxygen evolution reaction: from mechanistic understanding to reactor design. *Joule* 5 (7), 1704–1731. doi:10.1016/j.joule.2021.05.005

Doan, T., Lee, H., Shah, S., Kim, M., Kim, C., Cho, H. S., et al. (2021). A review of the porous transport layer in polymer electrolyte membrane water electrolysis. *Int. J. Energy Res.* 45 (10), 14207–14220. doi:10.1002/er.6739

Faid, A. Y., Xie, L., Barnett, A. O., Seland, F., Kirk, D., and Sunde, S. (2020). Effect of anion exchange ionomer content on electrode performance in AEM water electrolysis. *Int. J. hydrogen energy* 45 (53), 28272–28284. doi:10.1016/j.ijhydene.2020.07.202

Feng, Q., Liu, G., Wei, B., Zhang, Z., Li, H., Wang, H., et al. (2017). A review of proton exchange membrane water electrolysis on degradation mechanisms and mitigation strategies. *J. Power Sources* 366, 33–55. doi:10.1016/j.jpowsour.2017.09.006

Holzapfel, P. K., Bühler, M., Escalera-López, D., Bierling, M., Speck, F. D., Mayrhofer, K. J., et al. (2020). Fabrication of a robust PEM water electrolyzer based on non-noble metal cathode catalyst: [Mo3S13] 2− clusters anchored to N-doped carbon nanotubes. *Small* 16 (37), 2003161. doi:10.1002/smll.202003161

Ito, H., Maeda, T., Nakano, A., Hwang, C. M., Ishida, M., Kato, A., et al. (2012). Experimental study on porous current collectors of PEM electrolyzers. *Int. J. hydrogen energy* 37 (9), 7418–7428. doi:10.1016/j.ijhydene.2012.01.095

Ito, H., Maeda, T., Nakano, A., and Takenaka, H. (2011). Properties of Nafion membranes under PEM water electrolysis conditions. *Int. J. hydrogen energy* 36 (17), 10527–10540. doi:10.1016/j.ijhydene.2011.05.127

Knöppel, J., Möckl, M., Escalera-López, D., Stojanovski, K., Bierling, M., Böhm, T., et al. (2021). On the limitations in assessing stability of oxygen evolution catalysts using aqueous model electrochemical cells. *Nat. Commun.* 12 (1), 2231–2239. doi:10.1038/s41467-021-22296-9

Krivina, R. A., Ou, Y., Xu, Q., Twight, L. P., Stovall, T. N., and Boettcher, S. W. (2021). Oxygen electrocatalysis on mixed-metal oxides/oxyhydroxides: from fundamentals to membrane electrolyzer technology. *Accounts Mater. Res.* 2 (7), 548–558. doi:10.1021/accountsmr.1c00087

Kroschel, M., Bonakdarpour, A., Kwan, J. T. H., Strasser, P., and Wilkinson, D. P. (2019). Analysis of oxygen evolving catalyst coated membranes with different current collectors using a new modified rotating disk electrode technique. *Electrochimica Acta* 317, 722–736. doi:10.1016/j.electacta.2019.05.011

Lee, B. S., Park, H. Y., Choi, I., Cho, M. K., Kim, H. J., Yoo, S. J., et al. (2016). Polarization characteristics of a low catalyst loading PEM water electrolyzer operating at elevated temperature. *J. Power Sources* 309, 127–134. doi:10.1016/j.jpowsour.2015.12.139

Li, H., Fujigaya, T., Nakajima, H., Inada, A., and Ito, K. (2016b). Optimum structural properties for an anode current collector used in a polymer electrolyte membrane water electrolyzer operated at the boiling point of water. *J. Power Sources* 332, 16–23. doi:10.1016/j.jpowsour.2016.09.086

Li, H., Inada, A., Fujigaya, T., Nakajima, H., Sasaki, K., and Ito, K. (2016a). Effects of operating conditions on performance of high-temperature polymer electrolyte water electrolyzer. *J. Power Sources* 318, 192–199. doi:10.1016/j.jpowsour.2016.03.108

Li, H., Nakajima, H., Inada, A., and Ito, K. (2018). Effect of flow-field pattern and flow configuration on the performance of a polymer-electrolyte-membrane water electrolyzer at high temperature. *Int. J. Hydrogen Energy* 43 (18), 8600–8610. doi:10.1016/j.ijhydene.2018.02.171

Liu, J., and Weber, A. Z. (2022). Ionomer optimization for hydroxide-exchange-membrane water electrolyzers operated with distilled water: a modeling study. *J. Electrochem. Soc.* 169, 054506. doi:10.1149/1945-7111/ac69c4

Lopata, J., Kang, Z., Young, J., Bender, G., Weidner, J. W., and Shimpalee, S. (2020). Effects of the transport/catalyst layer interface and catalyst loading on mass and charge transport phenomena in polymer electrolyte membrane water electrolysis devices. *J. Electrochem. Soc.* 167 (6), 064507. doi:10.1149/1945-7111/ab7f87

Natarajan, V., Basu, S., and Scott, K. (2013). Effect of treatment temperature on the performance of RuO2 anode electrocatalyst for high temperature proton exchange membrane water electrolysers. *Int. J. hydrogen energy* 38 (36), 16623–16630. doi:10.1016/j.ijhydene.2013.05.133

Park, J. E., Kim, J., Han, J., Kim, K., Park, S., Kim, S., et al. (2021). High-performance proton-exchange membrane water electrolysis using a sulfonated poly (arylene ether sulfone) membrane and ionomer. *J. Membr. Sci.* 620, 118871. doi:10.1016/j.memsci.2020.118871

Pham, C. V., Escalera-López, D., Mayrhofer, K., Cherevko, S., and Thiele, S. (2021). Essentials of high performance water electrolyzers–from catalyst layer materials to electrode engineering. *Adv. Energy Mater.* 11 (44), 2101998. doi:10.1002/aenm.202101998

Siracusano, S., Baglio, V., Van Dijk, N., Merlo, L., and Aricò, A. S. (2017). Enhanced performance and durability of low catalyst loading PEM water electrolyser based on a short-side chain perfluorosulfonic ionomer. *Appl. energy* 192, 477–489. doi:10.1016/j.apenergy.2016.09.011

Stiber, S., Balzer, H., Wierhake, A., Wirkert, F. J., Roth, J., Rost, U., et al. (2021). Porous transport layers for proton exchange membrane electrolysis under extreme conditions of current density, temperature, and pressure. *Adv. Energy Mater.* 11 (33), 2100630. doi:10.1002/aenm.202100630

Su, H., Linkov, V., and Bladergroen, B. J. (2013). Membrane electrode assemblies with low noble metal loadings for hydrogen production from solid polymer electrolyte water electrolysis. *Int. J. hydrogen energy* 38 (23), 9601–9608. doi:10.1016/j.ijhydene.2013.05.099

Teuku, H., Alshami, I., Goh, J., Masdar, M. S., and Loh, K. S. (2021). Review on bipolar plates for low-temperature polymer electrolyte membrane water electrolyzer. *Int. J. Energy Res.* 45 (15), 20583–20600. doi:10.1002/er.7182

Thanasilp, S., and Hunsom, M. (2010). Effect of MEA fabrication techniques on the cell performance of Pt–Pd/C electrocatalyst for oxygen reduction in PEM fuel cell. *Fuel* 89, 3847–3852. doi:10.1016/j.fuel.2010.07.008

Wang, Y., Liao, X., Xu, H., He, W., Li, H., Xing, L., et al. (2023). Lattice Boltzmann simulation of cathode catalyst layer degradation on transport reaction process within a proton exchange membrane fuel cell. *Green Energy Resour.* 1, 100022. doi:10.1016/j.gerr.2023.100022

Wang, Y., Liu, T., Sun, H., He, W., Fan, Y., and Wang, S. (2020). Investigation of dry ionomer volume fraction in cathode catalyst layer under different relative humilities and nonuniform ionomer-gradient distributions for PEM fuel cells. *Electrochimica Acta* 353, 136491. doi:10.1016/j.electacta.2020.136491

Wang, Y., Wang, H., Wang, C., He, W., Zhao, Y., and Wang, X. (2024). Droplet flow characteristics on experimentally measured gas diffusion layer surfaces of polymer electrolyte membrane fuel cells. *J. Power Sources* 590, 233801. doi:10.1016/j.jpowsour.2023.233801

Wang, Y., Wang, S., Liu, S., Li, H., and Zhu, K. (2019). Three-dimensional simulation of a PEM fuel cell with experimentally measured through-plane gas effective diffusivity considering Knudsen diffusion and the liquid water effect in porous electrodes. *Electrochimica acta* 318, 770–782. doi:10.1016/j.electacta.2019.06.120

Wang, Y., Xu, H., Wang, X., Gao, Y., Su, X., Qin, Y., et al. (2022). Multi-sub-inlets at cathode flow-field plate for current density homogenization and enhancement of PEM fuel cells in low relative humidity. *Energy Convers. Manag.* 252, 115069. doi:10.1016/j.enconman.2021.115069

Xu, J., Aili, D., Li, Q., Christensen, E., Jensen, J. O., Zhang, W., et al. (2014). Oxygen evolution catalysts on supports with a 3-D ordered array structure and intrinsic proton conductivity for proton exchange membrane steam electrolysis. *Energy and Environ. Sci.* 7 (2), 820–830. doi:10.1039/c3ee41438h

Xu, J., Li, Q., Hansen, M. K., Christensen, E., García, A. L. T., Liu, G., et al. (2012). Antimony doped tin oxides and their composites with tin pyrophosphates as catalyst supports for oxygen evolution reaction in proton exchange membrane water electrolysis. *Int. J. hydrogen energy* 37 (24), 18629–18640. doi:10.1016/j.ijhydene.2012.09.156

Xu, W., and Scott, K. (2010). The effects of ionomer content on PEM water electrolyser membrane electrode assembly performance. *Int. J. Hydrogen Energy* 35 (21), 12029–12037. doi:10.1016/j.ijhydene.2010.08.055

Xu, W., Scott, K., and Basu, S. (2011). Performance of a high temperature polymer electrolyte membrane water electrolyser. *J. Power Soures* 196, 8918–8924. doi:10.1016/j.jpowsour.2010.12.039